Dynamic properties of cubic nonlinear Schrödinger equation with varying nonlinear parameter

2004 J. Phys. A: Math. Gen. 37 1589

(http://iopscience.iop.org/0305-4470/37/5/009)

INSTITUTE OF PHYSICS PUBLISHING JOURNAL OF PHYSICS A: MATHEMATICAL AND GENERAL

J. Phys. A: Math. Gen. **37** (2004) 1589–1602 PII: S0305-4470(04)65238-3

Dynamic properties of cubic nonlinear Schrödinger equation with varying nonlinear parameter

Xueshen Liu and Peizhu Ding

Institute of Atomic and Molecular Physics, Jilin University, Changchun, Jilin 130012, People's Republic of China

Received 20 June 2003, in final form 27 October 2003
Published 19 January 2004
Online at stacks.iop.org/JPhysA/37/1589 (DOI: 10.1088/0305-4470/37/5/009)

Abstract

The dynamic properties of the cubic nonlinear Schrödinger equation are investigated numerically using the symplectic scheme (Euler centred scheme). We discuss the dynamic behaviour of the cubic nonlinear Schrödinger equation with varying nonlinear parameter. The results show that the system exhibits regular recurrence for weakly nonlinearity. We also illustrate that the system will exhibit varying dynamic behaviour with increasing nonlinear parameter, i.e. the system will show the homoclinic orbit (HMO) crossing, quasi-recurrence, pseudorecurrence, irregular motion or stochastic motion for a strongly nonlinear constants.

PACS numbers: 02.60.Cb, 05.45.Pq, 45.20.−d

1. Introduction

It is well known that the nonlinear Schrödinger equation (NSE) with local cubic nonlinearity

$$\mathrm{i}\frac{\partial E}{\partial t} + \frac{\partial^2 E}{\partial x^2} + q|E|^2 E = 0 \tag{1}$$

has been used to describe many physical processes, such as nonlinear optics, plasma physics and fluid dynamics. For the cubic NSE (1), many works have been done analytically and numerically. Chang *et al* [1] presented a new linearized Crank–Nicholson-type scheme by applying an extrapolation technique to the real coefficient of the nonlinear term. A system of NSE that described the boson condensate under the mean-field approximation was numerically solved with a modified Crank–Nicholson scheme [2]. Tan and Mao [3] showed that the drifting of the solution pattern is a common phenomenon in the NSE. For generalized nonlinear Schrödinger equations, the nonlinear term $q|E|^2E$ can be extended to the general form of $f(|E|^2)E$, and the function $f(|E|^2)$ can be chosen as $f(|E|^2) = |E|^{2\alpha}$,

$$f(|E|^2) = |E|^2 - g|E|^4 \qquad f(|E|^2) = \frac{|E|^2}{1+g|E|^2} \quad \text{or} \quad f(|E|^2) = \frac{1}{2g}\left(1 - \mathrm{e}^{-2g|E|^2}\right)$$

0305-4470/04/051589+14$30.00

in different physical problems. In [4], Zhou *et al* obtained the pattern structure on generalized nonlinear Schrödinger equations with different nonlinear terms and discussed the spatiotemporal characteristics with various nonlinear terms in one- and two-dimensional spaces; they also showed that the high-order Hamiltonian perturbation can lead to the destruction of coherent structures and the formation of spatiotemporally complicated patterns. Moon [5] illustrated the correlations between a homoclinic orbit and coherent patterns in the nonlinear Schrödinger equation, and showed that irregular homoclinic orbit crossing can be observed corresponding to the chaotic oscillations if a perturbed term is added to the nonlinear Schrödinger equation. The basic behaviour of the high-order nonlinear Schrödinger equation involving cubic–quintic terms has also been discussed in [6]. The homoclinic structure in the nonlinear Schrödinger equation and coherence and chaos in the driven damped sine–Gordon equation have been studied in [7, 8]. Lemesurier *et al* [9] solved numerically the cubic and quintic nonlinear Schrödinger equations in two and three dimensions and also showed the universal properties.

It is easy to show that the cubic nonlinear Schrödinger equation (1) has three conserved quantities [10], i.e., the quasi-particle number

$$I_1 = \int |E|^2 \,\mathrm{d}x \tag{2}$$

the total momentum

$$I_2 = \frac{1}{2}\mathrm{i}\int (EE_x^* - E_xE^*)\,\mathrm{d}x \tag{3}$$

and the total energy

$$I_3 = \int \left(|E_x|^2 - \frac{q}{2}|E|^4\right)\,\mathrm{d}x. \tag{4}$$

In this paper, the NSE (1) is solved numerically using the symplectic scheme (Euler centred scheme). The basic dynamic properties of the NSE (1) are illustrated with varying nonlinear constant q, where q is in the range of 0.01–1.684. We show that the system will exhibit regular recurrence for weak nonlinearity and illustrate that strong nonlinearity will lead to varying dynamic behaviour which may be regular homoclinic orbit (HMO) crossing, irregular HMO crossing, quasi-recurrence or pseudorecurrence.

In section 2, the symplectic algorithm is extended to the calculations of the cubic nonlinear Schrödinger equation. First, the finite-dimensional canonical equation of the nonlinear Schrödinger equation is obtained by substituting a symmetry difference quotient for the two-order partial derivative. Then the canonical equations are computed using the symplectic scheme (Euler centred scheme). In section 3, the basic dynamic properties of the NSE (1) with varying nonlinear constant q are illustrated, and the conclusions and discussion are given in section 4.

2. Numerical recipe for the cubic nonlinear Schrödinger equation

As discussed in [2], the NSE can be rewritten in the Hamilton formalism with the standard transformation. Thus the NSE (1) has a symplectic structure, the evolution of the NSE (1) is a canonical transformation. Equation (1) is an infinite-dimensional Hamiltonian system. To illustrate the dynamic behaviour of the nonlinear Schrödinger equation, it is natural to look for an algorithm which preserves as much as possible the symplectic structure and the symmetries of the original continuous systems. A symplectic algorithm is an algorithm that preserves the symplectic structure of the Hamiltonian system [11–16], and thus is the natural and effective way to solve the NSE (1) numerically.

Let us now consider the NSE (1) with the following periodic boundary condition:

$$E(x+L) = E(x) \tag{5}$$

where L is the periodic length and $E(x,t)$ is the complex function denoting the wavefunction. If we divide the complex variable $E(x,t)$ of equation (1) into real and imaginary parts

$$E(x,t) = u(x,t) + \mathrm{i}v(x,t) \tag{6}$$

substitute the symmetry difference quotient for the two-order partial derivative

$$\frac{\partial^2 u_j}{\partial x^2} \approx \frac{1}{h^2}(u_{j-1} - 2u_j + u_{j+1}) \qquad \frac{\partial^2 v_j}{\partial x^2} \approx \frac{1}{h^2}(v_{j-1} - 2v_j + v_{j+1}) \tag{7}$$

and consider the period boundary condition (5), then the NSE (1) can be divided into the following finite-dimensional Hamiltonian canonical equations:

$$\frac{\mathrm{d}}{\mathrm{d}t}\begin{pmatrix} u \\ v \end{pmatrix} = J^{-1}\begin{pmatrix} \frac{\partial H}{\partial u} \\ \frac{\partial H}{\partial v} \end{pmatrix} \tag{8}$$

where space step $h = L/N$, N is a sufficiently large positive integer. We denote $x_j = jh$, $j = 0, 1, 2, \ldots, N, N+1$; $u_j = u_j(t) = u(x_j, t)$, $v_j = v_j(t) = v(x_j, t)$, the vector $u = (u_1, u_2, \ldots, u_N)^T$ and $v = (v_1, v_2, \ldots, v_N)^T$, '$T$' denotes the transposed matrix. The matrix J is the standard symplectic matrix which has the form

$$J = \begin{bmatrix} 0 & 1 \\ -1 & 0 \end{bmatrix}.$$

The Hamiltonian function of Hamiltonian canonical equations (8) is

$$H(u,v) = \frac{1}{2}(u^T \quad v^T)G\begin{pmatrix} u \\ v \end{pmatrix} + \frac{q}{4}\sum_{i=1}^{N}\left(u_i^2 + v_i^2\right)^2 \tag{9}$$

and

$$G = \begin{pmatrix} S & 0 \\ 0 & S \end{pmatrix} \qquad S = \frac{1}{h^2}\begin{bmatrix} -2 & 1 & 0 & \cdots & 0 & 1 \\ 1 & -2 & 1 & 0 & \cdots & 0 \\ 0 & 1 & -2 & 1 & \ddots & 0 \\ \vdots & \ddots & \ddots & \ddots & \ddots & 0 \\ 0 & \cdots & 0 & 1 & -2 & 1 \\ 1 & 0 & \cdots & 0 & 1 & -2 \end{bmatrix}$$

If we set $z = (u, v)^T$, the Hamiltonian canonical equation (8) can be written as

$$\frac{\mathrm{d}z}{\mathrm{d}t} = J^{-1}\frac{\partial H}{\partial z} = J^{-1}\nabla H \tag{10}$$

where $\frac{\partial H}{\partial z} = \nabla H = \left(\frac{\partial H}{\partial u}, \frac{\partial H}{\partial v}\right)^T$. The fundamental theorem on the Hamiltonian formalism says that the solution $z(t)$ of the canonical system (10) can be generated by a one-parameter group g_H^{0t}, depending on the given Hamiltonian H, of canonical transformation, where g_H^{0t} is a symplectic transformation, such that

$$z(t) = g_H^{0t} z(0). \tag{11}$$

That is to say that the solution of canonical equation (10) from t_1 to t_2 is a symplectic transformation $g_H^{t_1 t_2}$: $\binom{\varphi(t_2)}{\psi(t_2)} = g_H^{t_1 t_2}\binom{\varphi(t_1)}{\psi(t_1)}$. The time evolution of the Hamiltonian system (10) preserves the symplectic product conservation. Therefore, the symplectic algorithm is a reasonable method for solving the nonlinear Schrödinger equation. The second-order

Table 1. The evolution of the quasi-particle number (2) with time, where $\tau = 0.001$, $N = 64$ and $q = 1$.

Time	Conserved quantities (2)	Time	Conserved quantities (2)
0	6.314 601 233 508 811	500	6.314 601 233 508 901
10	6.314 601 233 508 824	600	6.314 601 233 508 911
100	6.314 601 233 508 872	700	6.314 601 233 508 877
200	6.314 601 233 508 923	800	6.314 601 233 508 904
300	6.314 601 233 508 907	900	6.314 601 233 508 906
400	6.314 601 233 508 924	950	6.314 601 233 508 878
450	6.314 601 233 508 877	1000	6.314 601 233 508 878

symplectic scheme based on the generating function [17] is

$$z^{k+1} = z^k + \tau J^{-1}(\nabla H)_{(\frac{z^{k+1}+z^k}{2})} \tag{12}$$

which is the well-known Euler centred scheme. The fourth-order symplectic scheme is

$$z^{n+1} = z^n + \tau J^{-1}(\nabla H)_{(\frac{z^{n+1}+z^n}{2})} - \frac{\tau^3}{24} J^{-1}\nabla_z((\nabla H)^T J H_{zz} J \nabla H)_{(\frac{z^{n+1}+z^n}{2})} \tag{13}$$

where τ is the time step and $\tau > 0$, $t_k = k\tau$, $k = 0, 1, 2, \ldots$, $u_j^k = u_j(t_k)$, $v_j^k = v_j(t_k)$, $u^k = \left(u_1^k u_2^k \cdots u_N^k\right)^T$, $v^k = \left(v_1^k v_2^k \cdots v_N^k\right)^T$ and $z^k = (u^k, v^k)^T$.
Since the symplectic schemes (12) and (13) are implicit schemes, we make use of an iteration method in each time step to compute the solutions.

3. Dynamic properties of the cubic nonlinear Schrödinger equation with varying nonlinear parameter

In the numerical computation, we choose the initial condition as

$$E(x, 0) = 1 + \varepsilon\, \mathrm{e}^{\mathrm{i}\theta} \cos(K_{\max} x). \tag{14}$$

This is a harmonically modulated initial wavefunction, where $K_{\max}$ is the unstable wave number corresponding to the maximum instability mode and $K_{\max} = 1$. ε is a small real constant which is chosen as $\varepsilon = 0.1$. $\varepsilon\, \mathrm{e}^{\mathrm{i}\theta}$ indicates the initial amplitude of the modulation. Moon [5] has investigated the long-time evolution of the NSE (1) for $q = 1$ when θ varied from 0° to 90° by means of numerical integration, and showed that there are two types of evolutionary patterns when θ varied from 0° to 45° and when θ varied from 45° to 90°. In this paper, we only consider the case that θ is slightly larger than 45° and choose $\theta = 45.18^\circ$. For a different nonlinear constant q, we study the NSE (1) under the periodic boundary condition (5) with the periodic length being taken as $L = 2\pi/K_{\max}$and the large positive integer $N = 64$.

The numerical solution of the cubic NSE (1) was obtained using the second-order symplectic scheme (12). In the computation, we choose the time step $\tau = 0.001$ and the computational time is from $t = 0$ to $t = 10^6$ (The long-time evolution is almost the same for $t > 1000$, thus we only discuss the dynamic properties for $0 \leqslant t \leqslant 1000$). The evolution of the quasi-particle number (2) with time for $q = 1$ is shown in table 1. It is shown that the conserved quantities are preserved to 10^{-12}. The symplectic method is as good as an iterative Crank–Nicholson scheme [2]. It is worth noting that the conserved quantities are preserved to 10^{-5} with the modified Crank–Nicholson scheme [2] and to 10^{-8} with the splitting time-step spectral method [6].

In order to analyse the dynamic properties of the cubic NSE (1) in a long-time evolution, we construct the phase-space diagrams (A, A_t) at $x = L/2$, which are defined as

$$\begin{cases} A(L/2, t) = |E(L/2, t)| - 1 \\ A_t(L/2, t) = \dfrac{\mathrm{d}A(L/2, t)}{\mathrm{d}t}. \end{cases} \tag{15}$$

For phase space $(A(L/2, t), A_t(L/2, t))$, Moon [5] experimentally guessed that the origin, $(A, A_t) = (0, 0)$, could be a saddle, and it was verified that the origin is the hyperbolic fixed point by linearized analysis [6] for $q = 1$. They also observed that a HMO would appear when θ is slightly larger than 45°.

In our numerical experiments, we consider the dynamic properties of the cubic nonlinear Schrödinger equation (1) with a varying nonlinear constant q under the initial condition (14), with q being in the range 0.01–1.684. For $q < 0.5$, the long-term behaviour of manifolds in phase space is only a single loop as shown in figures 1(a) and 2(a). The trajectories in the phase space are the elliptic orbit; it is verified that the origin, $(A, A_t) = (0, 0)$, could be an elliptic point. Figure 1(a) shows that the phase trajectories are of exact recurrence motion. Thus, the trajectories in phase space correspond to the periodic recurrence solutions for a small nonlinear constant q. When nonlinear constant q increases to 0.325 (figure 2(a)), the trajectories in phase space become thicker and no longer exactly periodic which corresponds to the quasi-recurrent solution. The time evolution of the amplitude of the fields $|E(x, t)|$at $x = L/2$ is periodically temporal evolution (figures 1(b) and 2(b)). The periodic behaviour can also be illustrated by the plot of the Fourier spectrum of $A(L/2, t)$with respect to time as seen in figures 1(c) and 2(c). Figure 1(c) shows that there is an isolated discrete distribution with equal frequency intervals. These characteristics exhibit that there exists an exactly periodic recurrence for weakly nonlinear parameter. Figures 1(d) and 2(d) display the contours of $|E(x, t)|^2 = \text{const}$, and exhibit regularly localized patterns. These phenomena verify the integrability of the cubic NSE (1). These numerical results illustrate that the trajectories in the phase space are a periodic recurrence orbit with coherent structure when we add a weak nonlinearity to them.

When we increase the constant q, the single loop in the phase space will shrink to the origin, $(A, A_t) = (0, 0)$, along the $A(L/2, t) = 0$ axis, and become two loops. Simultaneously the origin becomes a saddle. This phenomenon appears in the range $0.5 < q < 0.98$. When the constant q is in the range $0.9820 < q < 0.9840$, the centre point is similar to a small loop, and the periodic behaviour in phase space is shown in figure 3(a) for $q = 0.565$ and $q = 0.9825$. The quasi-recurrence or periodic recurrence solution is still exhibited in figures 3(b)–(d) for $q = 0.9825$. From the phase trajectories of figure 3(a) we can see that the HMO appears. It implies that the periodic trajectories may shift from the HMO to the near trajectories. The time-evolution of the amplitude of fields may appear chaotic. The large nonlinear constant q may lead to irregular HMO crossings, and the dynamic properties will exhibit stochastic behaviour.

Figure 4 shows a completely dynamic property for $q = 0.9945$. However, the irregular HMO crossing can be clearly seen in figure 4(a), and it is shown that the periodic orbit is broken up in phase space. The typically chaotic characteristic is exhibited by the temporal evolution of the amplitude of the fields (figure 4(b)). This illustrates that the irregular motion has appeared near the HMO and the integrability of the NSE (1) has broken down. From further analysis of figure 4(b) we can find that the amplitude of the fields looks like the quasi-recurrence for $t < 350$ and the trajectories in phase space are the regular HMO. Irregular HMO crossing appears for $t > 350$. The Fourier spectrum of $A(L/2, t)$ with respect to time clearly indicates that the broadband structure and noise-like spectrum are the chaotic time evolution

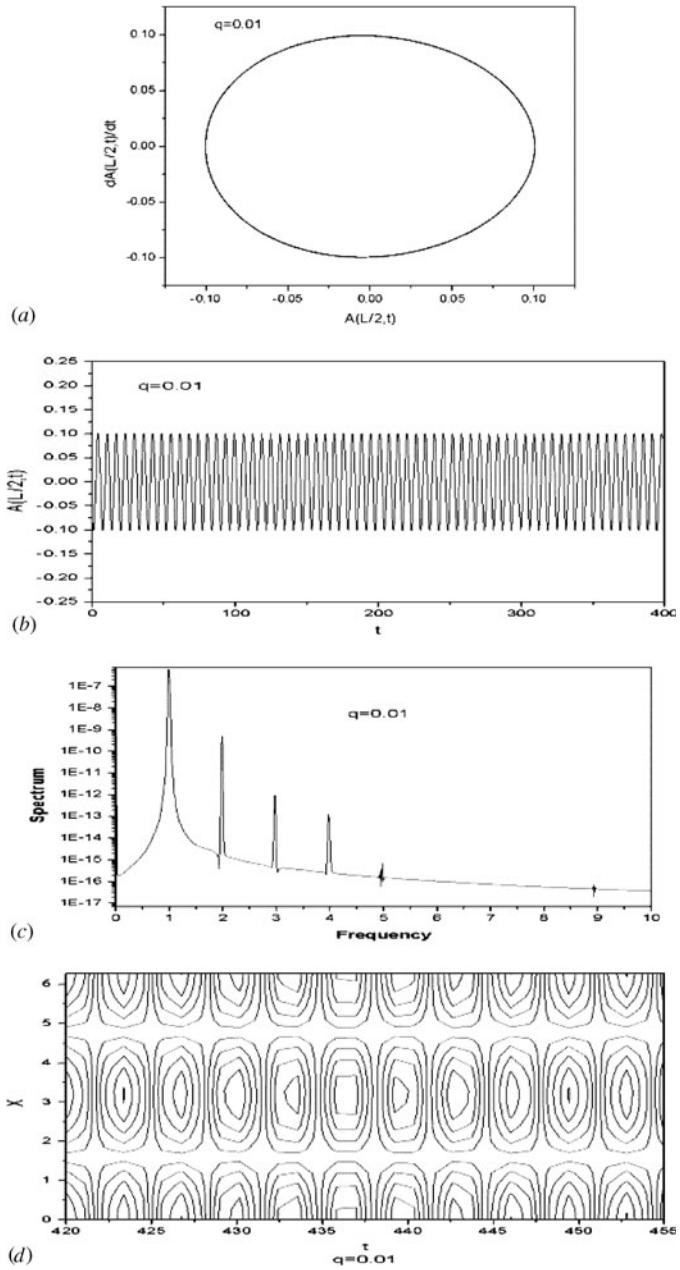

Figure 1. Solutions of the cubic nonlinear Schrödinger equation with $\theta = 45.18^\circ$ and $q = 0.01$. (*a*) Phase trajectories. (*b*) The time evolution of the amplitude of fields at $x = L/2$. (*c*) The Fourier spectrum of $A(L/2, t)$ with respect to time. (*d*) Contours of $|E(X, t)|^2 = \text{const}$, where $t = 420$–455 and $X = 0$–L.

(figure 4(*c*)). These phenomena illustrate the presence of stochastic motion for a complicated dynamic system. The contour of $|E(x, t)|^2 = \text{const}$ (figure 4(*d*)) indicates that the propagation velocity of the localized structure is not a constant. It again shows the presence of stochastic motion.

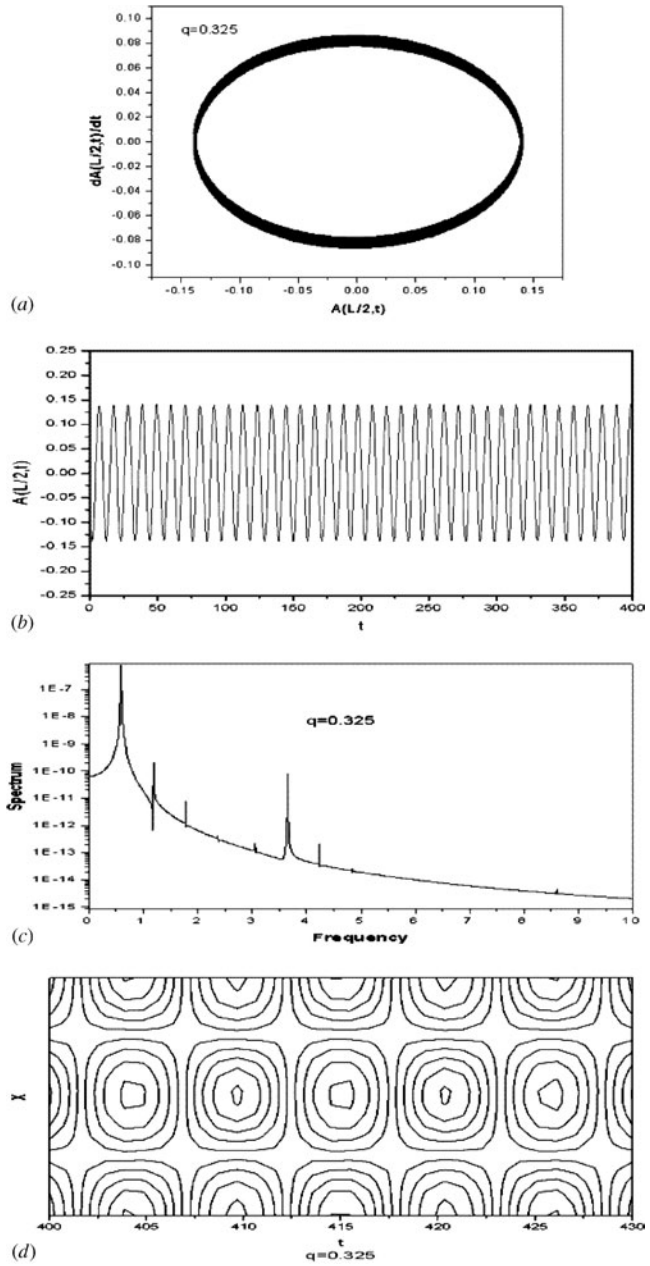

Figure 2. Solutions of the cubic nonlinear Schrödinger equation with $\theta = 45.18^\circ$ and $q = 0.325$. (*a*) Phase trajectories. (*b*) The time evolution of the amplitude of fields at $x = L/2$. (*c*) The Fourier spectrum of $A(L/2, t)$ with respect to time. (*d*) Contours of $|E(X, t)|^2 = \text{const}$, where $t = 400$–430 and $X = 0$–L.

As $q = 1.009$, it is worthwhile to note that the long-term behaviour of the manifolds in phase space again becomes a single loop starting from and back to the same saddle, $(A, A_t) = (0, 0)$, to form the Kolmogorov–Arnold–Moser (KAM) torus, and the KAM torus is very thick but is not destroyed. It indeed corresponds to the quasi-recurrence (figure 5(*a*)).

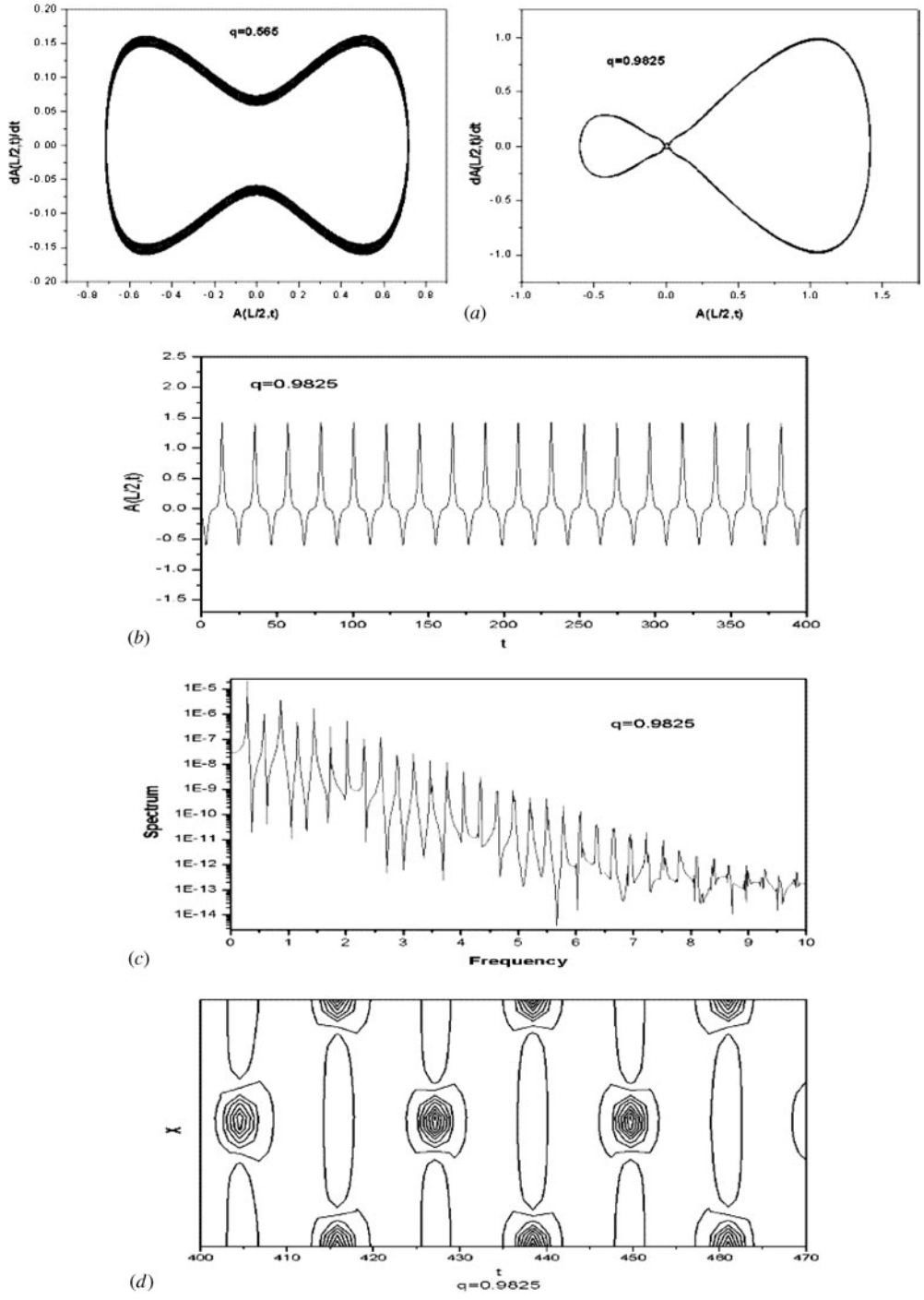

Figure 3. Solutions of the cubic nonlinear Schrödinger equation with $\theta = 45.18^\circ$ and $q = 0.565$ or $q = 0.9825$. (*a*) Phase trajectories. (*b*) The time evolution of the amplitude of fields at $x = L/2$. (*c*) The Fourier spectrum of $A(L/2, t)$ with respect to time. (*d*) Contours of $|E(X, t)|^2 = \text{const}$, where $t = 400$–470 and $X = 0$–L.

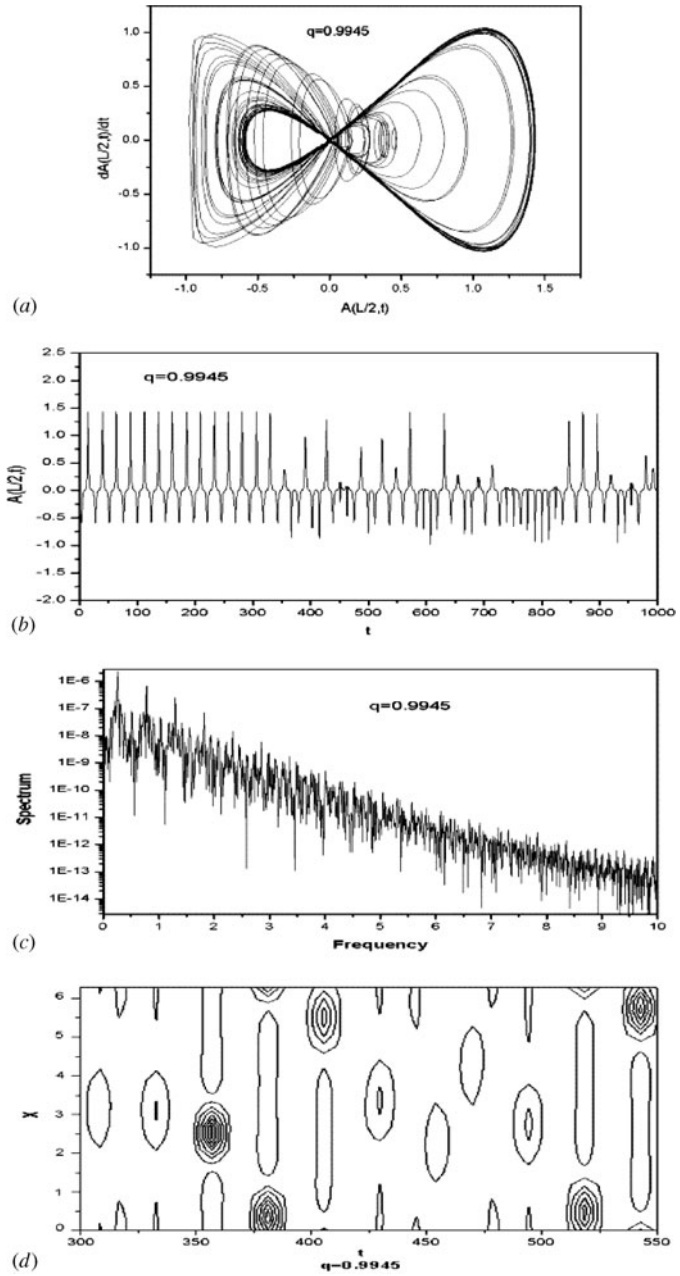

Figure 4. Chaotic trajectories of the cubic nonlinear Schrödinger equation with $\theta = 45.18^\circ$ and $q = 0.9945$. (*a*) Phase trajectories. (*b*) The time evolution of the amplitude of fields at $x = L/2$. (*c*) The Fourier spectrum of $A(L/2, t)$ with respect to time. (*d*) Contours of $|E(X, t)|^2 = \text{const}$, where $t = 300$–550 and $X = 0$–L.

If we continue to increase the nonlinear constant q till $q = 1.0115$, two-loop motion can be observed, and we think that the pseudorecurrence appears. The periodic recurrence can still be observed from the Fourier spectrum of $A(L/2, t)$ with respect to time, and the maximum peak of the power spectrum can also be exhibited. But there are some subharmonics in each of the

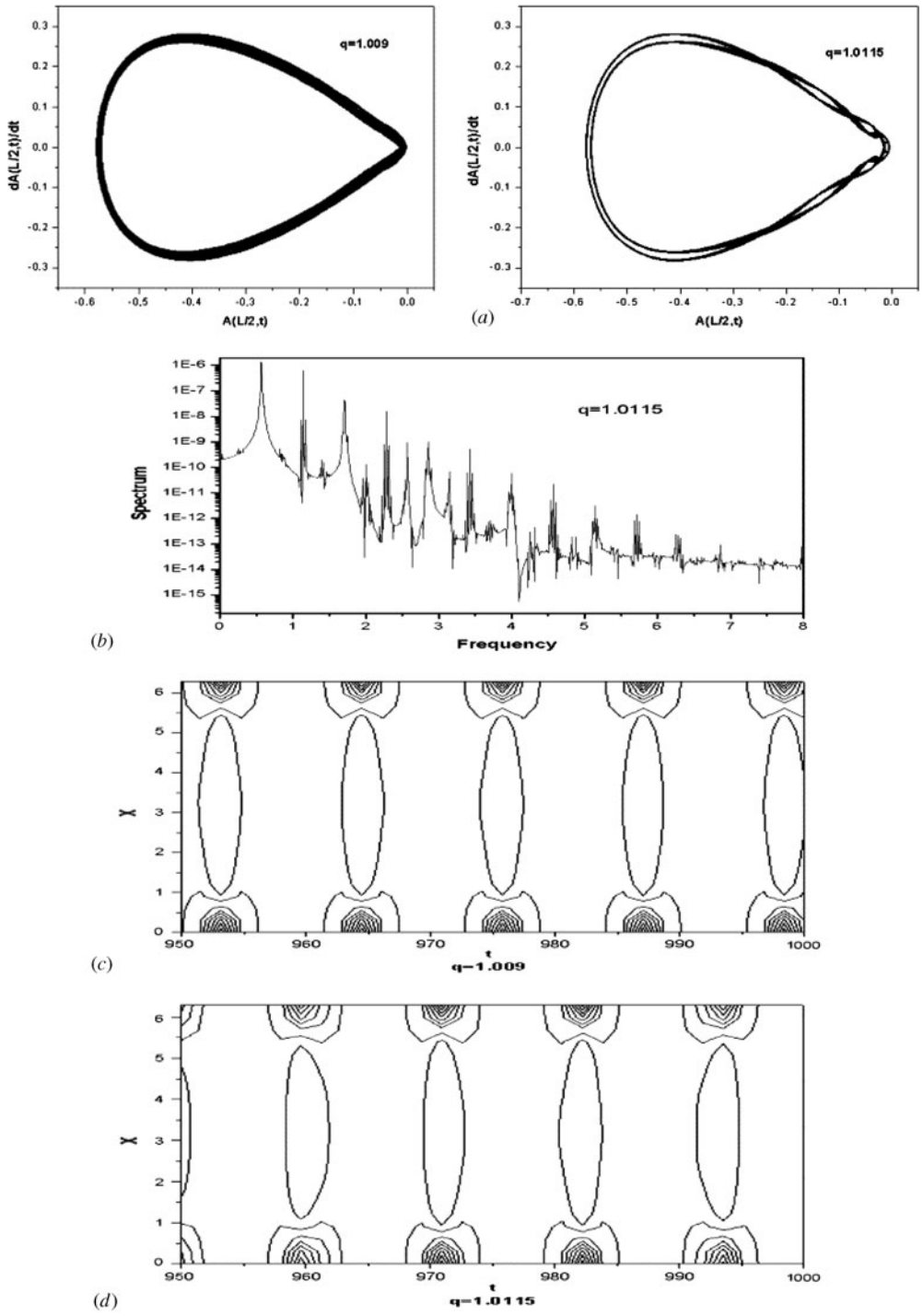

Figure 5. Solutions of the cubic nonlinear Schrödinger equation with $\theta = 45.18^\circ$ and $q = 1.009$ or $q = 1.0115$. (*a*) Phase trajectories. (*b*) The Fourier spectrum of $A(L/2, t)$ with respect to time. (*c*) Contours of $|E(X, t)|^2 = \text{const}$, where $t = 950$–1000 and $X = 0$–L. (*d*) Contours of $|E(X, t)|^2 = \text{const}$, where $t = 950$–1000 and $X = 0$–L.

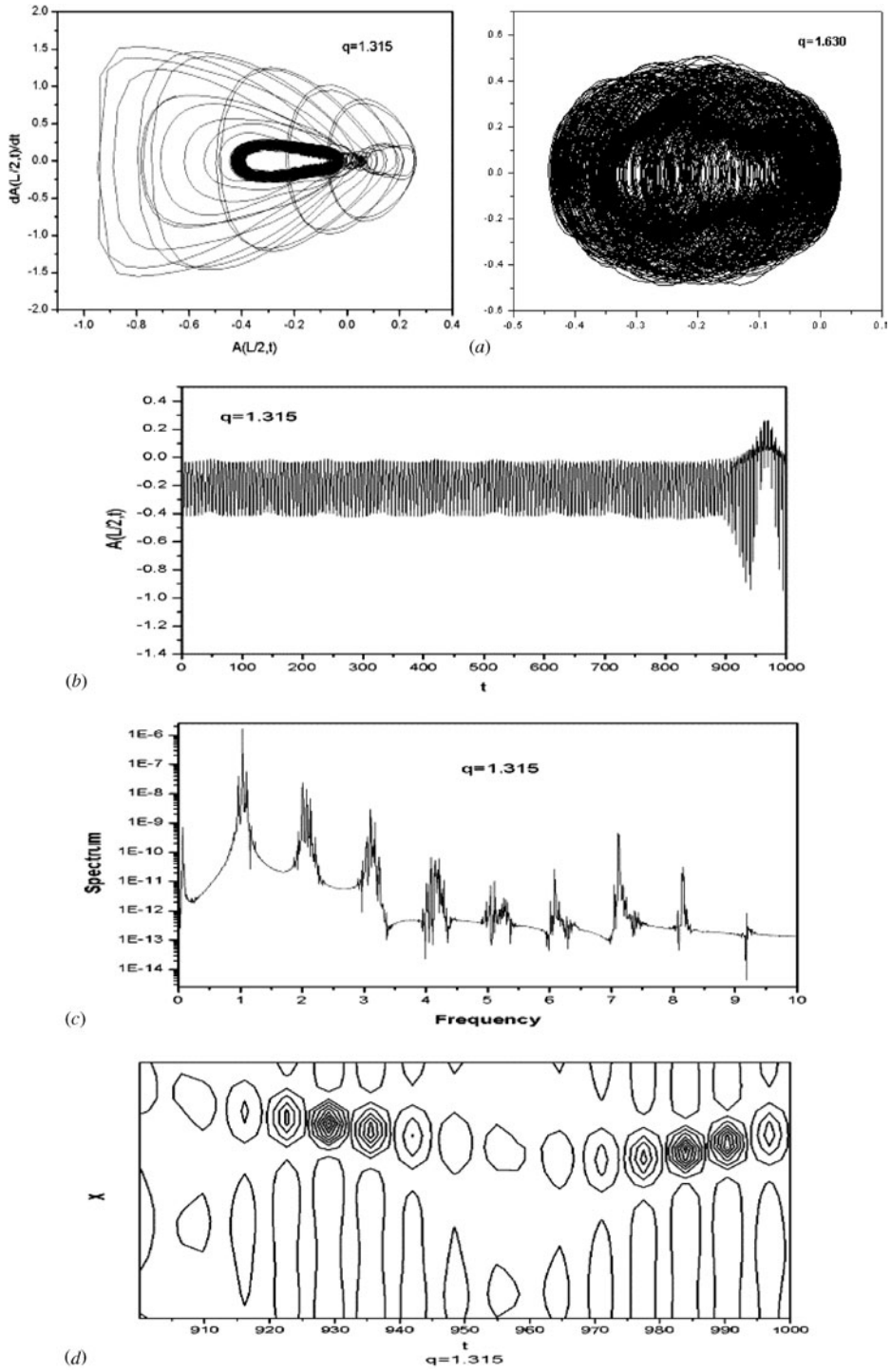

Figure 6. Chaotic trajectories of the cubic nonlinear Schrödinger equation with $\theta = 45.18^\circ$ and $q = 1.315$ or $q = 1.630$. (*a*) Phase trajectories. (*b*) The time evolution of the amplitude of fields at $x = L/2$. (*c*) The Fourier spectrum of $A(L/2, t)$ with respect to time. (*d*) Contours of $|E(X,t)|^2 =$ const, where $t = 900$–1000 and $X = 0$–L.

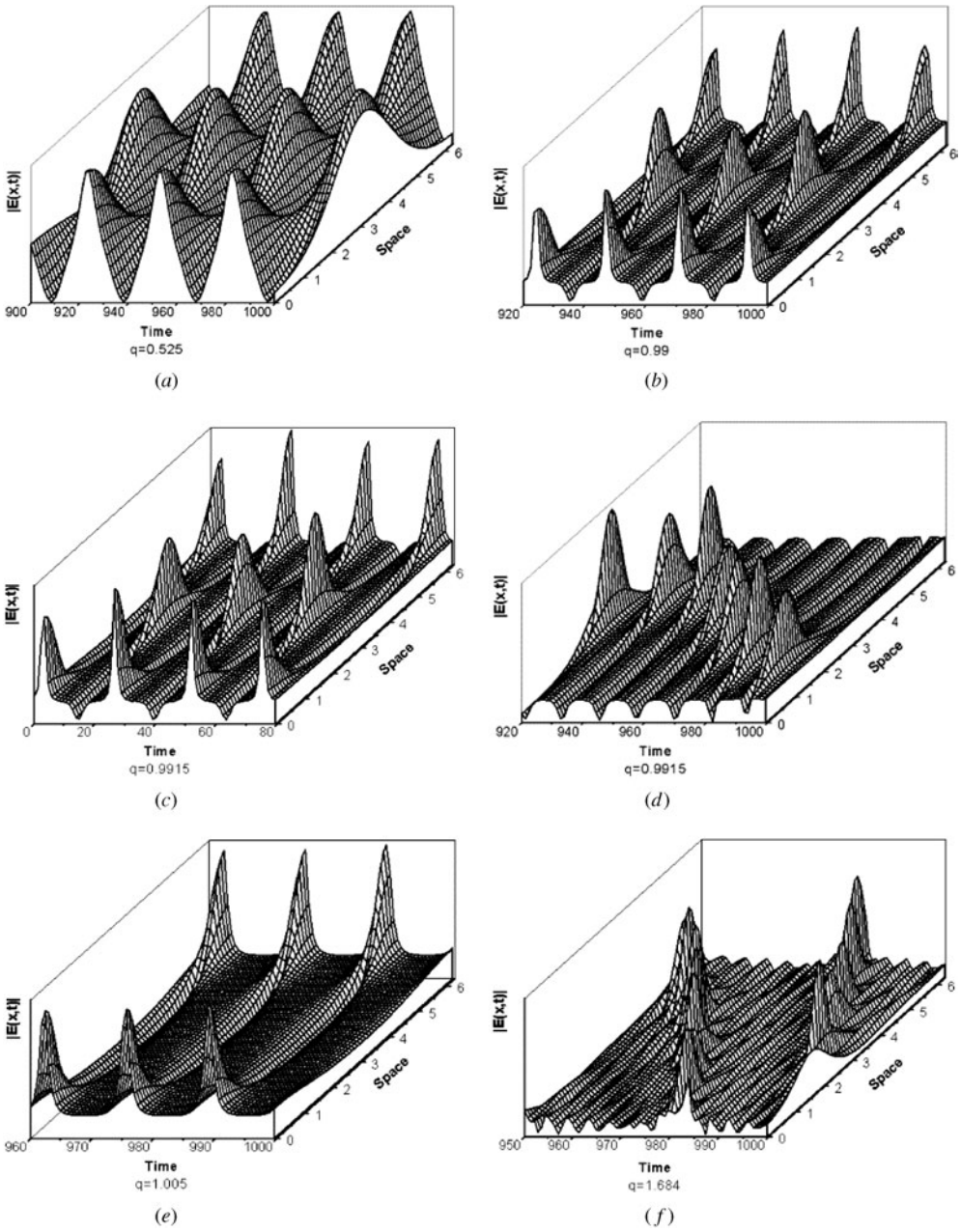

Figure 7. Spatially localized structure for a varying nonlinear constant.

maximum peaks of the power spectrum. These characteristics are shown in figure 5(*b*). We can see from figure 5(*c*) that the regularly localized pattern is formed as $q = 1.009$, and there is little irregular structure for the motion with two-cycle as $q = 1.0115$, as shown in figure 5(*d*). It illustrates the motion of the system from the periodic recurrence to the pseudorecurrence.

With the increase in the nonlinear constant q, the quasi-recurrent or pseudorecurrence in the phase space is again broken down. As $q = 1.315$ or $q = 1.630$, the evolution of the trajectories in a long time scale again exhibits irregular motion, as shown in figure 6(a). And the time evolution of the amplitude of field also exhibits stochastic behaviour as seen in figure 6(b). Figure 6(c) indicates that there are many subharmonics in each of the maximum peaks of the power spectrum. At the same time, the contours of $|E(x,t)|^2 =$ const as seen in figure 6(d) indicate that there are many irregularly localized patterns, which illustrate that the time evolution of the system is evolution with stochastic speed. These features show that the evolution of the spatial localized pattern will induce temporal chaos. Hence, from our numerical results, we can conclude that the route is as follows (with increasing nonlinear constant q): periodic recurrence with coherent structure (the origin in phase space is an elliptic point) $\rightarrow$ quasi-recurrence $\rightarrow$ regular HMO (the origin in phase space becomes a saddle) $\rightarrow$ irregular HMO $\rightarrow$ quasi-recurrence or pseudorecurrence $\rightarrow$ stochastic motion or irregular motion.

Finally, to illustrate the regular and stochastic motion with a different nonlinear constant q in the cubic NSE (1), we give the spatially localized structure in figure 7 for $q = 0.525$, 0.99, 0.9915, 1.005 and 1.684. Figure 7(a) shows the spatially localized structure for weak nonlinearity; one can observe the regular motion. When the nonlinear constant q is increased, this system will exhibit complex motion. When $0.6 \leqslant q \leqslant 0.99$, our numerical results show that a HMO will appear, but we still can see the recurrence from figure 7(b). Figures 7(c) and (d) show the spatially localized structure with $q = 0.9915$ for $0 \leqslant t \leqslant 80$ and $920 \leqslant t \leqslant 1000$. Figure 7($c$) is still exhibiting quasi-recurrence for $0 \leqslant t \leqslant 80$. But for long-time evolution the irregular HMO crossing can be observed from our numerical results, the irregular motion appears near the HMO and the dynamic properties exhibit stochastic behaviour (figure 7(d)). When q is in the range 1.005–1.009, we can observe in the phase space that there is a single loop starting from and back to the same saddle to form the KAM torus, it corresponds to quasi-recurrence, the same dynamic properties can be observed from the spatially localized structure (figure 7(e)). When $q \geqslant 1.01$, this system exhibits more complex dynamic behaviour, which may be pseudorecurrence, and then it may return to quasi-recurrence or one can observe stochastic motion. Figure 7(f) shows the irregular spatially localized structure for $q = 1.684$.

4. Discussions and conclusions

The basic dynamic behaviour of the cubic nonlinear Schrödinger equation is studied using the symplectic scheme with a varying nonlinear parameter. The numerical results illustrate that the system will preserve the regular recurrence with weak perturbation and the trajectories in the phase space are the elliptic orbit; the origin, $(A, A_t) = (0, 0)$, of the phase space is an elliptic point. When we increase the constant q, the periodic orbit in the phase space will shrink to the origin, $(A, A_t) = (0, 0)$, along the $A(L/2, t) = 0$ axis, and become two loops. Simultaneously the origin becomes a saddle when the nonlinear constant q is in the range $0.5 < q < 0.98$. The HMO will appear in the phase space. But the large nonlinear constant q ($0.9825 < q < 1.005$) may lead to regular or irregular HMO crossings, and the dynamic properties may exhibit stochastic behaviour. The motion of the system will change from periodic recurrence to pseudorecurrence and to chaos. When $q \geqslant 1.005$, the system will exhibit more complex dynamic behaviour which may be quasi-recurrence, pseudorecurrence or stochastic motion. These phenomena can also be seen clearly from the spatially localized structure.

The basic dynamic behaviour of the cubic nonlinear Schrödinger equation with a varying nonlinear parameter is very important in several branches of physics and mathematics. Reference [18] studied the stability of the stationary state of a mean-field Schrödinger equation with local cubic nonlinearity by a linear analysis, with the dynamics of the stationary state for different kinds of perturbations being discussed. It is well known that many physical phenomena can be explained using the cubic NSE (1), it is therefore very significant to study the different behaviour of the cubic NSE (1) with strong or weak nonlinearity.

Acknowledgments

This work was supported by The National Natural Science Foundation of China (10171039, 10074019) and The Special Funds for Major State Basic Research Projects (G1999032804).

References

[1] Chang Q S, Jia E and Sun W 1999 Difference schemes for solving the generalized nonlinear Schrödinger equation *J. Comput. Phys.* **148** 397–415
[2] Castiglioney P, Jona-Lasinioz G and Presilla C 1996 Spectral properties of quantum *N*-body systems versus chaotic properties of their mean-field approximations *J. Phys. A: Math. Gen.* **29** 6169–82
[3] Tan Y and Mao J M 2000 Drifting of the solution pattern for the nonlinear Schrödinger equation *J. Phys. A: Math. Gen.* **33** 9119–30
[4] Zhou C T, He X T and Cai T X 1994 Pattern structures on generalized nonlinear Schrödinger equations with various nonlinear terms *Phys. Rev.* E **50** 4136–55
[5] Moon H T 1990 Homoclinic crossings and pattern selection *Phys. Rev. Lett.* **64** 412–4
[6] Zhou C T, He X T and Chen S G 1992 Basic dynamic properties of high-order nonlinear Schrödinger equation *Phys. Rev.* A **46** 2277–85
[7] Overman E A II, Mclaughlin D W and Bishop A R 1986 Coherence chaos in the driven damped sine–Gordon equation: measurement of the soliton spectrum *Physica* D **19** 1–41
[8] Bishop A R, Mclaughlin D W, Forest M G and Overman E A II 1988 Quasi-periodic route to chaos in a near-integrable PDE: homoclinic crossings *Phys. Lett.* A **127** 335–40
[9] Lemesurier B J, Papanicplaou G, Sulem C and Sulem P L 1998 Focusing and multi-focusing solutions of the nonlinear Schrödinger equation *Physica* D **31** 78–102
[10] He X T 1982 Non-linear effect on the large amplitude waves interaction with particles of low frequency oscillation in plasma *Acta Phys. Sinica* **31** 1317–36 (in Chinese)
[11] Arnold V I 1978 *Mathematical Method of Classical Mechanics* (Berlin: Springer)
[12] Feng K 1986 Difference schemes for Hamiltonian formalism and symplectic geometry *J. Comput. Math.* **4** 279–89
[13] Sanz-Serna J M and Calvo M P 1994 *Numerical Hamiltonian Problem* (London: Chapman and Hall)
[14] Huang M Y, Qu R and Gong C C 1999 A structure-preserving discretization of nonlinear Schrödinger equation *J. Comput. Math.* **17** 553–60
[15] Liu X S, Su L W, Liu X Y and Ding P Z 2001 Numerical solution of a two-dimensional time-independent Schrödinger equation by using symplectic schemes *Int. J. Quant. Chem.* **83** 303–9
[16] Liu X S, Su L W and Ding P Z 2002 Symplectic algorithm for use in computing the time-independent Schrödinger equation *Int. J. Quant. Chem.* **87** 1–11
[17] Feng K, Wu H M, Qin M Z and Wang D L 1989 Construction of canonical difference schemes for Hamiltonian formalism via generating functions *J. Comput. Math.* **7** 71–96
[18] D'Agosta R and Presilla C 2002 States without a linear counterpart in Bose–Einstein condensates *Phys. Rev.* A **65** 043609